DOI : 10.1109/TIM.2008.917670

Laser Doppler Velocimetry for Joint Measurements of Acoustic and Mean Flow Velocities : LMS-based Algorithm and CRB Calculation

Laurent Simon, *Member, IEEE*, Olivier Richoux, Anne Degroot and Louis Lionet

Abstract

This paper presents a least mean square (LMS) algorithm for the joint estimation of acoustic and mean flow velocities from laser doppler velocimetry (LDV) measurements. The usual algorithms used for measuring with LDV purely acoustic velocity or mean flow velocity may not be used when the acoustic field is disturbed by a mean flow component. The LMS-based algorithm allows accurate estimations of both acoustic and mean flow velocities. The Cramér-Rao bound (CRB) of the associated problem is determined. The variance of the estimators of both acoustic and mean flow velocities is also given. Simulation results of this algorithm are compared with the CRB and the comparison leads to validate this estimator.

Index Terms

Laser Doppler Velocimetry, Acoustic Velocity, Mean Flow Velocity, Least Mean Square Method, Cramér-Rao Bound

Laser Doppler Velocimetry for Joint Measurements of Acoustic and Mean Flow Velocities : LMS-based Algorithm and CRB Calculation

I. Introduction

Laser Doppler Velocimeter (LDV) is an optical technique allowing direct measurement of local and instantaneous fluid velocity. This method is nonintrusive and is based on optical interferometry for estimating the velocity of scatterers suspended in a fluid by means of the frequency analysis of the light scattered by the seeding particles [1].

For fluid mechanics measurements, the particle velocity can be considered as constant during the transit time of the seeding particle through the measurement volume (defined by the interferometry fringes volume) and the frequency of the LDV signal is constant during this period [16]. Typical order of magnitude of mean flow velocities are from a few meters per second up to higher than the acoustic celerity (supersonic flow). The data processing consists then to estimate the power spectral density (PSD) of the velocity signal, from Poisson-based randomly distributed samples. PSD may be estimated by interpolating the randomly distributed samples, by resampling the interpolating signal and by compensating the effect of interpolation in the Fourier domain [5]- [20]. The autocorrelation function (ACF) may also be reconstructed from the randomly distributed samples and the Fourier transform of the estimated ACF gives an estimation of the PSD [11]. Lastly, Kalman filtering may be used for estimating the PSD [2].

For sine acoustic excitation, the particle velocity is no longer constant and the LDV signal is frequency modulated [21]- [10]. To estimate the particle velocity from these signals, specific signal processing techniques are used as spectral analysis [6], [22], [25], photon correlation [18] or frequency demodulation associated to post-processing methods [8], [23], [24]. Typical order of magnitude of mean flow velocities are from a few micrometers per second up to 100 millimeters per second, for frequencies in $[10 - 4000]$ Hz.

On one hand, for most acoustic measurements, the particle velocity can be considered as the sum of an AC-component due to acoustic excitation and a weak DC-contribution due to flow. When the particle oscillates in the measurement volume during further acoustic periods, the effect of the flow can be reduced and usual post-processing methods may be used [24]- [9].

On the other hand, the DC-flow component prevents in many cases the use of the post-processing methods given by [8], [23], [24], because the signal time length is less or largely less than one acoustic period. The aim of this paper is to estimate both the dc (flow) and ac (acoustic) components from such LDV signals.

Lazreq and Ville [13] measured the acoustic velocity in presence of mean flow by means of a probe consisting in a hot wire and a microphone. Their results showed a good agreement between the theory and the experiment but this probe cannot be considered as nonintrusive. LDV has also been used by adapting the slotting technique to estimate the acoustic particle velocity in a turbulent flow [15] with a 2D-LDV velocimeter. The acoustic impedance was estimated by means of a LDV probe and with a microphone probe and the different results were compared. Finally, Boucheron *et al* [4] has developed a new method of signal processing called 'perio-correlation' in order to estimate sine acoustic velocity in strong mean flow by LDV.

In this work, the sine acoustic excitation is supposed to be perfectly known and a frequency demodulation technique [8] is performed to estimate the particle velocity from the LDV signal. In this paper, we propose a new method to estimate jointly the acoustic particle velocity (amplitude and phase) and the mean flow velocity from the velocity signal. This method is based on the least mean square (LMS) algorithm. The mean flow velocity, the amplitude and phase of acoustic particle velocity are estimated for each seeding particle crossing the measurement volume. Furthermore, the Cramér-Rao bound (CRB) of the associated problem is calculated. The CRB gives the lowest variance of any unbiased estimator and consequently yields theoretically the minimum uncertainties linked to the velocity estimations (acoustic and mean flow velocities). Lastly, simulated data are processed, in order to validate the LMS-based algorithm and to compare the variance of the results with the Cramér-Rao bound.

Section II deals with the LDV principles including the velocity signal modeling and the associated signal processing for acoustic applications. In section III, the data processing based on the least mean square algorithm is explained and the Cramér-Rao bound of both the mean flow and acoustic velocities are determined. Finally, the results of the Monte Carlo simulation are shown and compared to the Cramér-Rao bounds in section IV, for acoustic frequencies in $[125 - 4000]$ Hz, for acoustic velocities in $[0.05 - 50]$ mm.s^{-1} and for mean flow velocities in $[0.05 - 5000]$ mm.s^{-1}.

II. Fundamentals of Laser Doppler Velocimetry

In this section, we consider time-varying signals such that $t \in [t_q - T_q/2, t_q + T_q/2]$, t_q being the central time of the signal, T_q being a time of flight, and q being associated to a given seeding particle.

A. Laser Doppler Velocimetry Principle

In the differential mode, two coherent laser beams are crossed and focused to generate an ellipsoidal probe volume, in which the electromagnetic interferences lead to apparent dark and bright fringes [1].

The velocity $v_q(t)$ of the seeding particle denoted q is related to the scattered optical field due to the Doppler effect. The light intensity scattered by the particle crossing the probe volume is modulated in amplitude and frequency. The frequency of modulation $F_q(t)$ is called Doppler frequency and is given by

$$F_q(t) = \frac{v_q(t)}{i} = \frac{2v_q(t)}{\lambda_L} \sin(\theta/2), \tag{1}$$

where $v_q(t)$ is the velocity of the particle along the x-axis, i the fringe-spacing expressed as a function of the angle θ between the incoming laser beams and their optical wavelength λ_L (Fig. 1).

The diffused light is collected by a receiving optics and is converted into an electrical signal by a photomultiplier (PM). This signal can then be modelled as [8]

$$s_q(t) = A_q(t)(M + \cos\phi_q(t)), \tag{2}$$

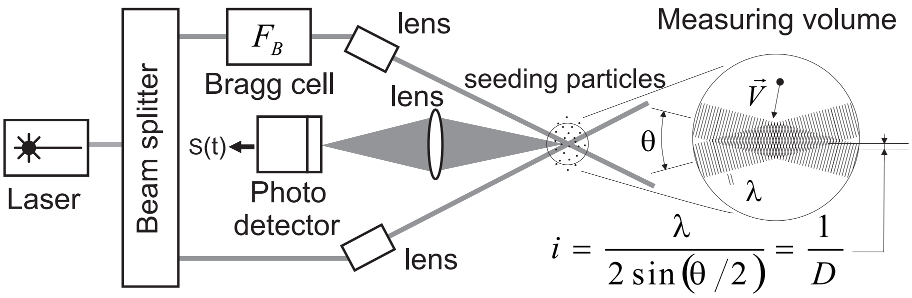

Fig. 1. Optical setup of LDV system. When the particle q crosses the measurement volume, the light is scattered in all directions and the burst signal $s_q(t)$ is collected by the photo detector. Data processing of $s_q(t)$ allows then to estimate the mean flow and particle acoustic velocity.

where M takes into account the positive sign of Cramér-Rao Bound (CRB) the light intensity. In (2), the amplitude modulation linked to the normally distributed light intensity across the beam section is written as

$$A_q(t) = K_q e^{-(\beta d_q(t))^2}, \tag{3}$$

where K_q is related to the laser beam, the PM sensitivity, the electronic amplification, the observation direction and the scattering efficiency of tracer q. Furthermore, β is related to the probe geometry and $d_q(t)$ is the projection of the time-varying particle displacement along the x-axis in the probe volume. Similarly, the phase modulation in (2) is described by

$$\phi_q(t) = 2\pi\frac{d_q(t)}{i} + \phi_0, \tag{4}$$

where ϕ_0 is the initial phase due to optical setup. Furthermore, we denote $x_q(t)$ the signal such that

$$x_q(t) = s_q(t) + w(t), \tag{5}$$

where $w(t)$ is the additive noise [24].

In order to avoid any ambiguity on the sign of the velocity, a Bragg cell tuned to frequency $F_B = 40$ MHz is used to shift the frequency of one of the lasers. The signal $s_q(t)$ is consequently written as

$$s_q(t) = A_q(t)(M + \cos(2\pi F_B t + 2\pi d_q(t)/i + \phi_0)). \tag{6}$$

The offset component M is then canceled by an high-pass filtering and the signal $s_q(t)$ is down shifted to zero thanks to a quadrature demodulation (QD) technique [14]. The actual signal, called burst signal, can finally be written as

$$s_q(t) = A_q(t)\cos(2\pi d_q(t)/i + \phi_0). \tag{7}$$

B. Doppler Signal Modeling in Acoustics

Considering only pure sine acoustic waves and supposing that the mean flow velocity is constant inside the probe volume, the projection along the x-axis of the velocity of a particle q subjected jointly to the sine acoustic wave and the mean flow field can be expressed as

$$v_q(t) = v_{c,q} + V_{ac}\cos(2\pi F_{ac} t + \phi_{ac}), \tag{8}$$

where $v_{c,q}$ is the mean flow velocity of particle q, V_{ac} and ϕ_{ac} are the amplitude and phase of the acoustic particle velocity and F_{ac} is the known frequency of the pure sine acoustic excitation. The amplitude modulation of the burst signal (3) associated to the particle q may be written as

$$A_q(t) = K_q \exp[\beta(v_{c,q}(t-t_q) + \frac{V_{ac}}{2\pi F_{ac}} \sin(2\pi F_{ac} t + \phi_{ac}))]^2. \tag{9}$$

Similarly, the phase modulation (4) of the burst signal associated to the particle q is

$$\phi_q(t) = \frac{2\pi}{i} v_{c,q}(t-t_q) + \frac{V_{ac}}{2\pi F_{ac}} \sin(2\pi F_{ac} t + \phi_{ac}). \tag{10}$$

We note that the flow velocity $v_{c,q}$ can change from a particle q to another while the acoustic parameters v_{ac} and ϕ_{ac} are independent of q. Thus, when the acoustic wave is disturbed by a mean flow, assuming that the particles q cross the measurement volume at different random central times t_q, without time overlapping between bursts q and $q+1$, the Doppler signal can be written as

$$s(t) = \sum_q s_q(t) = A_D(t) \cos[\phi_D(t)], \tag{11}$$

where the amplitude and phase respectively express as

$$A_D(t) = \begin{cases} A_q(t), \ t \in [t_q - T_q/2, t_q + T_q/2] \\ 0, \text{otherwise}, \end{cases} \tag{12}$$

and

$$\phi_D(t) = \begin{cases} \phi_q(t), \ t \in [t_q - T_q/2, t_q + T_q/2] \\ 0, \text{otherwise}. \end{cases} \tag{13}$$

Furthermore, the time of flight of the tracer q is defined as [7]

$$T_q = \frac{\sqrt{2} D_x}{v_{c,q}}, \tag{14}$$

where D_x is the length of the probe volume in the x-axis and the associated number of acoustic periods is

$$N_{per} = \frac{\sqrt{2} D_x}{v_{c,q}} F_{ac}. \tag{15}$$

As expected, the fastest the particle crosses the probe volume, the lowest the time of flight and the number of acoustic periods. An example of a typical Doppler signal is shown on Fig. 2(a), where the different particle times of flight are associated to different mean flow velocities.

C. Doppler signal processing

The aim of the signal processing developed after sampling the Doppler signal is to estimate jointly and burst-by-burst the acoustic particle velocity (amplitude V_{ac} and phase ϕ_{ac}) and the mean flow velocity $v_{c,q}$. This procedure is usually split into two stages. After a detection procedure [7], a frequency demodulation of the Doppler signal $s(t)$ is performed by using a

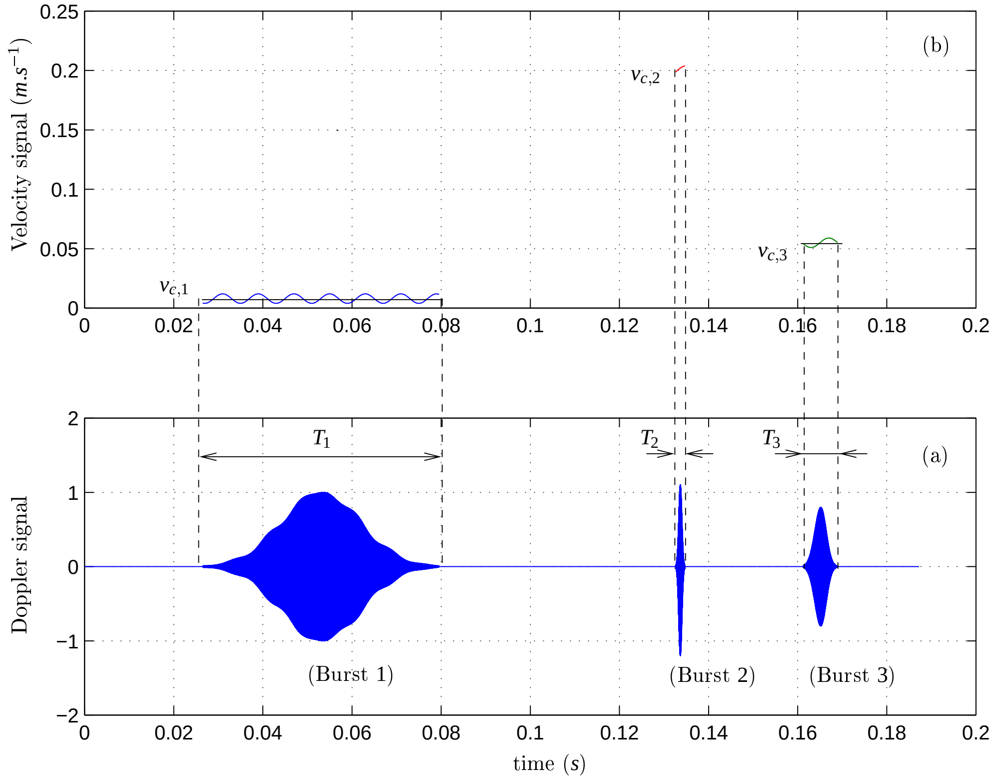

Fig. 2. (a) Example of a Doppler signal. (b) Associated velocity signal. Burst 1 is associated with a low mean flow velocity corresponding to N_{per} acoustic periods largely higher than 1. Burst 2 is associated with a high mean flow velocity corresponding to N_{per} acoustic period largely lower than 1. Burst 3 is associated to a mean flow velocity corresponding to $N_{per} \lesssim 1$ acoustic period.

time-frequency transform to estimate the instantaneous frequency $F_q(t)$, or equivalently (1) the velocity signal $v_q(t)$, burst by burst [23]. Note that the detector selects only bursts corresponding to one tracer in the measurement volume. Secondly, the data processing of the estimated velocity signal $\hat{v}_q(t)$ allows to obtain both components of the acoustic and mean flow velocities for each burst. This first stage is described in this subsection and the second one (data LMS-based processing) is explained in the section IV.

According to (1), the velocity signal associated to the particle q expresses as

$$v_q(t) = iF_q(t), \tag{16}$$

where i is the fringe spacing. Thus, the problem consists to estimate the mean value $\hat{v}_{c,q}$, the amplitude $\hat{V}_{ac}$ and the phase $\hat{\phi}_{ac}$ of the estimated velocity signal associated to each burst q from the actual noisy burst signal $x_q(t)$. Fig. 2 shows an example of an noiseless simulated Doppler signal (a) and the associated velocity signal for three non-overlapping bursts (b).

In section III, the Cramér Rao bound of the problem is calculated. Then, a method based on a least mean square algorithm is presented in section IV and is applied to simulated velocity signals $v_q(t)$ in section V.

III. CRB CALCULATION

We recall that the Cramér-Rao bound (CRB) gives the lowest bound of the variance an unbiased estimator may reach (if it exists) [12]. As explained in [12], the CRB alerts us to the physical impossibility of finding an unbiased estimator whose variance is less than the bound. In the case of single tone signals, CRB were calculated by Rife and Boorstyn [17] in 1974. The CRB of LDV signals were also studied in the case of fluid mechanics [3]- [19]. In the case of sine acoustic excitation, the CRB of LDV signal were also studied by Le Duff [14].

We focus here on the problem of calculating the Cramér-Rao bound (CRB) of the following problem. The velocity data are assumed to be such that

$$u[n] = v[n;\theta] + w[n], \tag{17}$$

for $n \in [n_0, n_1]$, where $w[n]$ is the WGN, $w[n] \sim \mathcal{N}(0, \sigma^2)$, the data being modeled according to

$$v[n;\theta] = v_c + V_{ac}\cos(2\pi f_{ac} n + \phi_{ac}), \tag{18}$$

where $f_{ac} = F_{ac}/F_s$, F_s being the sampling frequency, $v_c \equiv v_{c,q}$, and where the unknown parameters are gathered in

$$\theta = [v_c \quad V_{ac} \quad \phi_{ac}]^T. \tag{19}$$

We furthermore suppose that $f_{ac} \neq 0$ and $f_{ac} \neq \frac{1}{2}$.

A. Cramér-Rao bound (CRB) for one burst

The CRB is given by the inverse of the Fisher information matrix $\mathbf{J}(\theta)$, $\mathrm{CRB}(\theta) = \mathbf{J}(\theta)^{-1}$, where the Fisher information matrix is given by [12]

$$\mathbf{J}(\theta)_{kl} = \frac{1}{\sigma^2}\sum_{n=n_0}^{n_1} \frac{\partial v[n;\theta]}{\partial \theta_k}\frac{\partial v[n;\theta]}{\partial \theta_l}, \tag{20}$$

for $k, l \in [1, 3]$, for $\theta = [v_c \quad V_{ac} \quad \phi_{ac}]^T$. The derivatives in (20), according to (18), lead to

$$\mathbf{J}(\theta) = \frac{1}{\sigma^2}\begin{pmatrix} N & \frac{\cos(\beta)\sin(\gamma N)}{\sin(\gamma)} & -\frac{V_{ac}\sin(\beta)\sin(\gamma N)}{\sin(\gamma)} \\ \frac{\cos(\beta)\sin(\gamma N)}{\sin(\gamma)} & \frac{N}{2} + \frac{\cos(2\beta)\sin(2\gamma N)}{2\sin(2\gamma)} & -\frac{V_{ac}\sin(2\beta)\sin(2\gamma N)}{2\sin(2\gamma)} \\ -\frac{V_{ac}\sin(\beta)\sin(\gamma N)}{\sin(\gamma)} & -\frac{V_{ac}\sin(2\beta)\sin(2\gamma N)}{2\sin(2\gamma)} & \frac{NV_{ac}^2}{2} - \frac{V_{ac}^2\cos(2\beta)\sin(2\gamma N)}{2\sin(2\gamma)} \end{pmatrix}, \tag{21}$$

where $N = n_1 - n_0 + 1$, and where

$$\gamma = \pi f_{ac}, \tag{22}$$

$$\beta = 2\pi f_{ac} n_0 + \pi f_{ac}(N-1) + \phi_{ac}. \tag{23}$$

We define the linear signal-to-noise ratio (SNR) of the velocity signal as

$$\mathrm{SNR} = \frac{V_{ac}^2}{2\sigma^2}, \tag{24}$$

and we then have upon inversion

$$\mathrm{var}(v_c) \geq \mathrm{CRB}(v_c) = \frac{V_{ac}^2}{4\ \mathrm{SNR}} \frac{N^2 - \left(\frac{\sin(2\gamma N)}{\sin(2\gamma)}\right)^2}{\frac{N^3}{2} - \frac{N}{2}\left(\frac{\sin(2\gamma N)}{\sin(2\gamma)}\right)^2 - N\left(\frac{\sin(\gamma N)}{\sin(\gamma)}\right)^2 + \frac{\sin(2\gamma N)}{\sin(2\gamma)}\left(\frac{\sin(\gamma N)}{\sin(\gamma)}\right)^2}, \tag{25}$$

$$\mathrm{var}(V_{ac}) \geq \mathrm{CRB}(V_{ac}) = \frac{V_{ac}^2}{2\ \mathrm{SNR}} \frac{N^2 - N\cos(2\beta)\frac{\sin(2\gamma N)}{\sin(2\gamma)} - 2\sin^2(\beta)\left(\frac{\sin(\gamma N)}{\sin(\gamma)}\right)^2}{\frac{N^3}{2} - \frac{N}{2}\left(\frac{\sin(2\gamma N)}{\sin(2\gamma)}\right)^2 - N\left(\frac{\sin(\gamma N)}{\sin(\gamma)}\right)^2 + \frac{\sin(2\gamma N)}{\sin(2\gamma)}\left(\frac{\sin(\gamma N)}{\sin(\gamma)}\right)^2}, \tag{26}$$

$$\mathrm{var}(\phi_{ac}) \geq \mathrm{CRB}(\phi_{ac}) = \frac{1}{2\ \mathrm{SNR}} \frac{N^2 + N\cos(2\beta)\frac{\sin(2\gamma N)}{\sin(2\gamma)} - 2\cos^2(\beta)\left(\frac{\sin(\gamma N)}{\sin(\gamma)}\right)^2}{\frac{N^3}{2} - \frac{N}{2}\left(\frac{\sin(2\gamma N)}{\sin(2\gamma)}\right)^2 - N\left(\frac{\sin(\gamma N)}{\sin(\gamma)}\right)^2 + \frac{\sin(2\gamma N)}{\sin(2\gamma)}\left(\frac{\sin(\gamma N)}{\sin(\gamma)}\right)^2}. \tag{27}$$

B. Cramér-Rao Bound (CRB) for N_b bursts

We now assume that the algorithm developed in III-A is used for estimating the unknown parameters $\theta = [v_c \quad V_{ac} \quad \phi_{ac}]^T$, in the case of N_b bursts. The main difference between this problem and the one developed above is that the index n_0 is not anymore a constant, but might be modeled as a discrete random variable, uniformly distributed in $[0, N_{ac}]$, where $N_{ac} = \mathrm{nint}\left[F_s/F_{ac}\right]$, nint[] being the nearest integer. As a consequence, the discrete random variable β given in (23), which appears in (26-27) is uniformly distributed in $[\pi(N-1)f_{ac} + \phi_{ac}, \pi(N-1)f_{ac} + \phi_{ac} + 2\pi]$. Averaging the terms linked to β in (26) and (27) consequently leads to

$$< \cos(2\beta) >=< \sin(2\beta) >= 0, \tag{28}$$

and

$$< \cos^2(\beta) >=< \sin^2(\beta) >= \frac{1}{2}. \tag{29}$$

This finally yields

$$\mathrm{var}(V_{ac}) \geq \mathrm{CRB}(V_{ac}) = \frac{V_{ac}^2}{2\ \mathrm{SNR}} \frac{N^2 - \left(\frac{\sin(\gamma N)}{\sin(\gamma)}\right)^2}{\frac{N^3}{2} - \frac{N}{2}\left(\frac{\sin(2\gamma N)}{\sin(2\gamma)}\right)^2 - N\left(\frac{\sin(\gamma N)}{\sin(\gamma)}\right)^2 + \frac{\sin(2\gamma N)}{\sin(2\gamma)}\left(\frac{\sin(\gamma N)}{\sin(\gamma)}\right)^2} \tag{30}$$

and

$$\mathrm{var}(\phi_{ac}) \geq \mathrm{CRB}(\phi_{ac}) = \frac{1}{2\ \mathrm{SNR}} \frac{N^2 - \left(\frac{\sin(\gamma N)}{\sin(\gamma)}\right)^2}{\frac{N^3}{2} - \frac{N}{2}\left(\frac{\sin(2\gamma N)}{\sin(2\gamma)}\right)^2 - N\left(\frac{\sin(\gamma N)}{\sin(\gamma)}\right)^2 + \frac{\sin(2\gamma N)}{\sin(2\gamma)}\left(\frac{\sin(\gamma N)}{\sin(\gamma)}\right)^2}. \tag{31}$$

In the following, we use the expressions (25) for v_c and (30) for V_{ac} for studying the CRB of the problem. We recall that N depends on v_c (36). As a consequence, the CRB of v_c (25) and the CRB of V_{ac} (30) both depend on v_c and V_{ac}, while the CRB of ϕ_{ac} (31) is independent of V_{ac}.

C. Asymptotic behavior of Cramér-Rao Bound (CRB)

In Appendix II, we give the expressions of the asymptotic CRB of θ, for both cases $2\gamma N \ll 1$ ($N_{per} \ll 1/(2\pi)$) and $2\gamma N \gg 1$ ($N_{per} \gg 1/(2\pi)$).

In the asymptotic case $2\gamma N \ll 1$, we prove (63-64) that the relative variance of v_c and V_{ac} are

$$\frac{\text{var}(v_c)}{v_c^2} \geq \frac{\text{CRB}(v_c)}{v_c^2} = \frac{1}{\text{SNR}} \frac{45}{\pi^4 2^{7/2}} \frac{1}{D_x^5 F_s} \frac{v_c^3 V_{ac}^2}{F_{ac}^4}, \tag{32}$$

$$\frac{\text{var}(V_{ac})}{V_{ac}^2} \geq \frac{\text{CRB}(V_{ac})}{V_{ac}^2} = \frac{1}{\text{SNR}} \frac{45}{\pi^4 2^{9/2}} \frac{1}{D_x^5 F_s} \frac{v_c^5}{F_{ac}^4}. \tag{33}$$

Both CRBs of v_c and V_{ac} are proportional to $v_c^5 V_{ac}^2$ and inversely proportional to F_{ac}^4. Consequently, doubling the mean flow velocity yields an 15 dB increase of the variance of both v_c and V_{ac}. Similarly, doubling the amplitude of the acoustic particle velocity V_{ac} leads to a 6 dB increase of the variance of both v_c and V_{ac}. Lastly, doubling the frequency of the pure sine acoustic wave leads to a 12 dB decrease of the variance of both v_c and V_{ac}. We also note that doubling the length of the probe volume D_x yields a 15 dB decrease of the variance of both v_c and V_{ac}.

In the asymptotic case $2\gamma N \gg 1$, we prove that (72-73)

$$\text{var}(v_c) \geq \frac{1}{\text{SNR}} \frac{1}{2^{3/2} D_x F_s} v_c V_{ac}^2, \tag{34}$$

and

$$\text{var}(V_{ac}) \geq \frac{1}{\text{SNR}} \frac{1}{\sqrt{2} D_x F_s} v_c V_{ac}^2. \tag{35}$$

Thanks to the exact (25, 30, 31) and asymptotic (32-35) expressions of the CRB, the minimum uncertainties linked to the velocity estimations (acoustic and mean flow velocities) are completely known. In section (IV), the LMS-based algorithm is introduced. It is then applied in section (V) to simulated data in order to be compared with the CRB.

IV. Least mean square algorithm

From a practical point of view, the actual velocity signal is uniformly sampled. Consequently, the number of samples N_q associated to the particle q is derived from (14), as

$$N_q = \frac{\sqrt{2} D_x F_s}{v_{c,q}}, \tag{36}$$

and the associated number of acoustic periods (15) is now defined as

$$N_{per} = \frac{\sqrt{2} D_x}{v_{c,q}} F_{ac}. \tag{37}$$

The sine-wave fit is then solved by minimizing the cost function $V(\theta)$,

$$V(\theta) = \frac{1}{N} \sum_{n=n_0}^{n_1} \left(u[n] - v[n;\theta]\right)^2, \tag{38}$$

with respect to the unknown parameters θ (19), where $u[n]$ and $v[n;\theta]$ are respectively given by (17) and (18), and where $N = n_1 - n_0 + 1$. In the Appendix 1, the equations (50-52) respectively give the expression of v_c, $a_{ac} = V_{ac}\cos(\phi_{ac})$ and $b_{ac} = V_{ac}\sin(\phi_{ac})$ as a function of $\mathbf{u}$ and f_{ac}. Once a_{ac} and b_{ac} are estimated, the unknown acoustical parameters of θ express as

$$\begin{cases} \hat{V}_{ac} = \sqrt{\hat{a}_{ac}^2 + \hat{b}_{ac}^2}, \\ \hat{\phi}_{ac} = \text{atan}\frac{\hat{b}_{ac}}{\hat{a}_{ac}}. \end{cases} \tag{39}$$

V. Numerical results and discussion

In this section, we compare the CRB with the LMS-based algorithm developed in IV. According to the values of the acoustic and mean flow velocities to be analyzed, the following values for F_{ac} and V_{ac} are chosen :

$$F_{ac} \in [125 \quad 250 \quad 500 \quad 1000 \quad 2000 \quad 4000] \text{ Hz}, \tag{40}$$

$$V_{ac} \in [0.05 \quad 1.58 \quad 50] \text{ mms}^{-1}. \tag{41}$$

The phase ϕ_{ac} is supposed to be equal to $\pi/4$, and we use an adimensional parameter α_v for the value of v_c, such that

$$\alpha_v = \frac{V_{ac}}{v_c} \in [0.01 \quad 0.05 \quad 0.1 \quad 0.5 \quad 1]. \tag{42}$$

For each numerical simulation, the sampling frequency is $F_s = 350$ kHz, the probe volume length along the $x-$axis is $D_x = 0.1$ mm and 10000 bursts are analyzed. The simulator is performed by Matlab.

Fig. 3 to Fig. 5 show typical results of the relative variances var$(v_c)/v_c^2$ (a) and var$(V_{ac})/V_{ac}^2$ (b), for the different values of F_{ac} with comparison to the theoretical CRB of v_c (25) and of V_{ac} (26). Each figure is related to a given value of F_{ac}. Furthermore, for each value of F_{ac}, three sets of signals are analyzed, each set corresponding to one of the bursts of Fig. 2, respectively $N_{per} \gg 1$ (Burst 1), $N_{per} > 1$ (Burst 2) and $N_{per} \lesssim 1$ (Burst 3), where N_{per} is the number of acoustic periods, $N_{per} = N f_{ac}$.

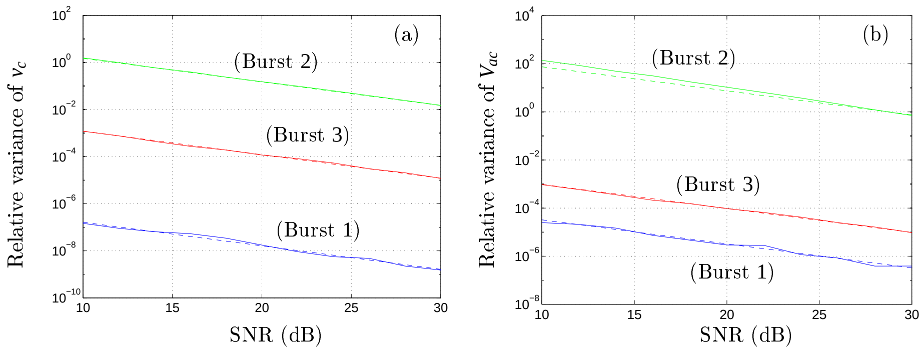

Fig. 3. Comparison of the relative variances of v_c (a) and V_{ac} (b) estimated by a LMS algorithm (continuous) with the theoretical CRB (dashed), for $F_{ac} = 125$ Hz. Bursts $(1-3)$ refer to Fig. 2. (Burst 1) : $V_{ac} = 1.58$ mm.s^{-1}, $\alpha_v = 0.1$, $v_c = 15.8$ mm.s^{-1}. (Burst 2) : $V_{ac} = 50$ mm.s^{-1}, $\alpha_v = 0.1$, $v_c = 500$ mm.s^{-1}. (Burst 3) : $V_{ac} = 50$ mm.s^{-1}, $\alpha_v = 1$, $v_c = 50$ mm.s^{-1}.

First of all, the LMS-based estimator is near the theoretical CRB, so that we can maintain that this estimator is efficient. Moreover, the relative variance of v_c is weaker than the one of V_{ac} (except for $\alpha_v = 1$). Indeed, for values of v_c and V_{ac} such

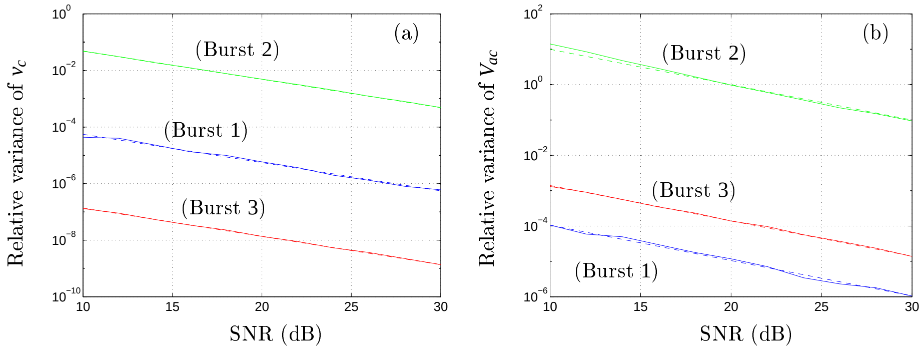

Fig. 4. Comparison of the relative variances of v_c (a) and V_{ac} (b) estimated by a LMS algorithm (continuous) with the theoretical CRB (dashed), for $F_{ac} = 500$ Hz. Bursts $(1-3)$ refer to Fig. 2. (Burst 1) : $V_{ac} = 50$ mm.s^{-1}, $\alpha_v = 1$, $v_c = 50$ mm.s^{-1}. (Burst 2) : $V_{ac} = 50$ mm.s^{-1}, $\alpha_v = 0.05$, $v_c = 1000$ mm.s^{-1}. (Burst 3) : $V_{ac} = 1.58$ mm.s^{-1}, $\alpha_v = 0.1$, $v_c = 15.8$ mm.s^{-1}.

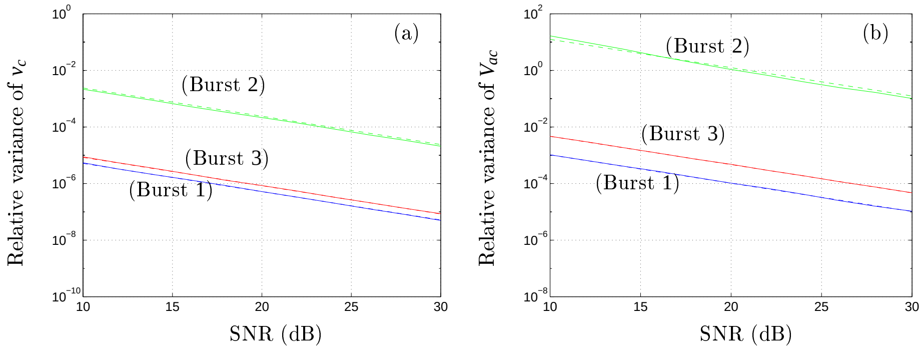

Fig. 5. Comparison of the relative variances of v_c (a) and V_{ac} (b) estimated by a LMS algorithm (continuous) with the theoretical CRB (dashed), for $F_{ac} = 4000$ Hz. Bursts $(1-3)$ refer to Fig. 2. (Burst 1) : $V_{ac} = 50$ mm.s^{-1}, $\alpha_v = 0.1$, $v_c = 500$ mm.s^{-1}. (Burst 2) : $V_{ac} = 50$ mm.s^{-1} , $\alpha_v = 0.01$, $v_c = 5000$ mm.s^{-1}. (Burst 3) : $V_{ac} = 50$ mm.s^{-1}, $\alpha = 0.05$, $v_c = 1000$ mm.s^{-1}.

that $\alpha_v = V_{ac}/v_c \leq 1/\sqrt{2}$ as $\mathrm{CRB}(v_c) \simeq \mathrm{CRB}(V_{ac})/2$, we have

$$\frac{\mathrm{CRB}(v_c)}{v_c^2} \leq \frac{\mathrm{CRB}(V_{ac})}{V_{ac}^2}. \tag{43}$$

Moreover, the values of the relative variances of v_c and V_{ac} drastically depend on the values of v_c, V_{ac} and F_{ac} as shown by (25) and (30).

- For $N_{per} > 1$ (Burst 1), the relative variances of v_c and V_{ac} are respectively in $[-70, -42]$ dB and $[-52, -30]$ dB. Such estimations may consequently be considered as very accurate.
- For $N_{per} \ll 1$ (Burst 2), the relative variances of v_c and V_{ac} are respectively in $[-27, 1]$ dB and $[10, 20]$ dB. The estimation of v_c is accurate enough for low values of $v_c^3 V_{ac}^2 / F_{ac}^4$ (32), while the estimation of V_{ac} is clearly unacceptable, whatever the parameters v_c, V_{ac} and F_{ac} (33).
- For $N_{per} \lesssim 1$ (Burst 3), the relative variances of v_c and V_{ac} are respectively in $[-70, -30]$ dB and $[-30, -23]$ dB. Such estimations may also be considered as very accurate.

Furthermore, for velocity signals with time length largely lower than one acoustic period, we can use the asymptotic case expression of CRB of v_c and V_{ac}. Giving a maximum value of relative error, respectively E_{v_c} for v_c and $E_{v_{ac}}$ for V_{ac}, we consequently have

$$\frac{\text{CRB}(v_c)}{v_c^2} = \frac{1}{\text{SNR}} \frac{45}{\pi^4 2^{7/2}} \frac{1}{D_x^5 F_s} \frac{v_c^3 V_{ac}^2}{F_{ac}^4} \leq E_{v_c} \tag{44}$$

and

$$\frac{\text{CRB}(V_{ac})}{V_{ac}^2} = \frac{1}{\text{SNR}} \frac{45}{\pi^4 2^{9/2}} \frac{1}{D_x F_s} \frac{v_c^5}{F_{ac}^4} \leq E_{v_{ac}}. \tag{45}$$

As a consequence, for a given set of setup known parameters D_x, F_s and F_{ac}, we may give the maximum values $v_c^3 V_{ac}^2$ and v_c^5 have to reach for yielding an error less than respectively E_{v_c} and $E_{v_{ac}}$.

Lastly, from the expressions of the CRB of v_c (25) and V_{ac} (30), we can calculate the number of acoustic periods the time length of the velocity signals may have, for leading to an error less than a given value E. Tables I-III give a summary of such results. Each table corresponds to a given burst of Fig. 2.

TABLE I

NUMBER OF ACOUSTIC PERIODS N_{per} (FOR v_c AND FOR V_{ac}) LEADING TO AN ERROR LESS THAN $E(\%)$ FOR $F_{ac} = 125$ HZ AND $V_{ac} = 50$ MM.S^{-1}.

SNR (dB)	10			20			30		
E (%)	0.1	1	10	0.1	1	10	0.1	1	10
N_{per} (v_c)	≥ 0.8	≥ 0.3	≥ 0.2	≥ 0.45	≥ 0.2	≥ 0.09	≥ 0.3	≥ 0.12	≥ 0.05
N_{per} (V_{ac})	$\gg 10$	≥ 0.75	≥ 0.25	$\gg 5$	≥ 0.5	≥ 0.2	≥ 0.8	≥ 0.25	≥ 0.1

TABLE II

NUMBER OF ACOUSTIC PERIODS N_{per} (FOR v_c AND FOR V_{ac}) LEADING TO AN ERROR LESS THAN $E(\%)$ FOR $F_{ac} = 500$ HZ AND $V_{ac} = 1.58$ MM.S^{-1}.

SNR (dB)	10			20			30		
E (%)	0.1	1	10	0.1	1	10	0.1	1	10
N_{per} (v_c)	≥ 0.4	≥ 0.16	≥ 0.06	≥ 0.25	≥ 0.1	≥ 0.04	≥ 0.18	≥ 0.06	≥ 0.02
N_{per} (V_{ac})	$\gg 10$	≥ 6	≥ 0.4	$\gg 10$	≥ 0.75	≥ 0.25	$\gg 5$	≥ 0.9	≥ 0.15

TABLE III

NUMBER OF ACOUSTIC PERIODS N_{per} (FOR v_c AND FOR V_{ac}) LEADING TO AN ERROR LESS THAN $E(\%)$ FOR $F_{ac} = 4000$ HZ AND $V_{ac} = 50$ MM.S^{-1}.

SNR (dB)	10			20			30		
E (%)	0.1	1	10	0.1	1	10	0.1	1	10
N_{per} (v_c)	≥ 0.6	≥ 0.25	≥ 0.1	≥ 0.4	≥ 0.15	≥ 0.05	≥ 0.25	≥ 0.1	≥ 0.03
N_{per} (V_{ac})	$\gg 20$	$\gg 5$	≥ 0.6	$\gg 10$	≥ 4.5	≥ 0.04	$\gg 10$	≥ 0.7	≥ 0.25

For example, table I may be read as follows. To obtain a relative error for v_c less than 0.1 % for SNR= 10 dB, the minimum number of acoustic period for the velocity signal is 0.8. In the same way, to obtain a relative error for V_{ac} less than 1 % for SNR= 20 dB, the minimum number of acoustic period for the velocity signal is 0.5. Tables II-III give the minimum number of acoustic periods the velocity signal should have for obtaining relative errors less than 0.1 %, 1 % and 10 %, for SNR equals to 10 dB, 20 dB and 30 dB for 500 Hz and 4000 Hz respectively.

As expected, the mean flow velocity v_c is estimated with a great accuracy from a very low number of acoustic period. For example, to obtain a relative error of 1 % for v_c, the number of acoustic period is always less than 0.3 whatever the SNR, F_{ac} and V_{ac}. On contrary, the results for the estimation of the acoustic velocity are much more contrasted. For a SNR of 30 dB, the estimation of V_{ac} associated with a relative error less than 1 % is possible for a number of acoustic period $N_{per} > 0.9$. But, when the SNR is less than 30 dB, the number of acoustic periods associated with a relative error less than 1 % may be largely bigger than 1.

The tables also show the influence of the acoustic frequency on the estimation of the particle acoustic velocity. The higher the frequency, the higher the number of acoustic periods for an accurate estimation of V_{ac}. For a relative error equals to 10 %, the number of acoustic periods are the same whatever the frequency. But for a relative error equals to 1 % or 0.1 % the estimation of the particle acoustic velocity is easier for a low frequency. On contrary, the influence of the frequency on the estimation of the mean flow velocity is the opposite. The higher the frequency, the lower the number of the acoustic periods for an accurate estimation.

With regard to the results of these study, a three-steps new approach can be proposed to improve the estimation of the acoustic particle velocity in presence of mean flow. The first step consists in the estimation of the mean flow velocity for each burst with the least mean square (LMS) algorithm. Then, the estimation of the mean flow velocity may be subtracted from the velocity signal. Finally, a ”rotating machinery” technique associated with a synchronous detection allows to estimate the acoustic particle velocity with a great accuracy [9].

VI. Conclusion

A new method for estimating jointly the acoustic particle and the mean flow velocities from a LDV signal is presented. It is based on the least mean square (LMS) algorithm and it performs well in the estimation of the velocities. The performance of the method has been investigated by means of numerical tests and the results of the simulation have been compared to the Cramér-Rao bounds of the associated problem. It is shown that the LMS-based estimator is near the theoretical CRB, so that the estimator is efficient.

Appendix I

Derivation of LMS problem

Inserting (18) into (38) leads to

$$V(\theta) = \frac{1}{N}\sum_{n=n_0}^{n_1}\Big(u_n - (v_c + a_{ac}\cos(2\pi f_{ac}n) + b_{ac}\sin(2\pi f_{ac}n)\Big)^2, \tag{46}$$

where

$$\begin{cases} a_{ac} = V_{ac}\cos(\phi_{ac}), \\ b_{ac} = V_{ac}\sin(\phi_{ac}). \end{cases} \tag{47}$$

Solving the following linear problem

$$\begin{cases} \frac{\partial V(\theta)}{\partial v_c} = 0, \\ \frac{\partial V(\theta)}{\partial V_{ac}} = 0, \\ \frac{\partial V(\theta)}{\partial \phi_{ac}} = 0, \end{cases} \tag{48}$$

allows to write analytically the unknown parameters. In the following, we note

$$\begin{aligned} D \;=\; & \frac{1}{N^2}\sum_{n=n_0}^{n=n_1}\cos^2(2\pi f_{ac}n)\sum_{n=n_0}^{n=n_1}\sin^2(2\pi f_{ac}n) - \frac{1}{N^2}\Big(\sum_{n=n_0}^{n=n_1}\cos(2\pi f_{ac}n)\sin(2\pi f_{ac}n)\Big)^2 \\ & -\frac{1}{N^3}\sum_{n=n_0}^{n=n_1}\sin^2(2\pi f_{ac}n)\Big(\sum_{n=n_0}^{n=n_1}\cos(2\pi f_{ac}n)\Big)^2 - \frac{1}{N^3}\sum_{n=n_0}^{n=n_1}\cos^2(2\pi f_{ac}n)\Big(\sum_{n=n_0}^{n=n_1}\sin(2\pi f_{ac}n)\Big)^2 \\ & +\frac{2}{N^3}\sum_{n=n_0}^{n=n_1}\cos(2\pi f_{ac}n)\sin(2\pi f_{ac}n)\sum_{n=n_0}^{n=n_1}\cos(2\pi f_{ac}n)\sum_{n=n_0}^{n=n_1}\sin(2\pi f_{ac}n). \end{aligned} \tag{49}$$

The mean flow velocity $\bar{v}$ may then be written as

$$\begin{aligned} v_c \;=\; & \frac{1}{N^3 D}\Big(\sum_{n=n_0}^{n=n_1}\sin(2\pi f_{ac}n)\sum_{n=n_0}^{n=n_1}\cos(2\pi f_{ac}n)\sin(2\pi f_{ac}n) - \sum_{n=n_0}^{n=n_1}\cos(2\pi f_{ac}n)\sum_{n=n_0}^{n=n_1}\sin^2(2\pi f_{ac}n)\Big)\sum_{n=n_0}^{n=n_1}u_n\cos(2\pi f_{ac}n) \\ & +\frac{1}{N^3 D}\Big(\sum_{n=n_0}^{n=n_1}\cos(2\pi f_{ac}n)\sum_{n=n_0}^{n=n_1}\cos(2\pi f_{ac}n)\sin(2\pi f_{ac}n) - \sum_{n=n_0}^{n=n_1}\sin(2\pi f_{ac}n)\sum_{n=n_0}^{n=n_1}\cos^2(2\pi f_{ac}n)\Big)\sum_{n=n_0}^{n=n_1}u_n\sin(2\pi f_{ac}n) \\ & +\frac{1}{N^3 D}\Big(\sum_{n=n_0}^{n=n_1}\cos^2(2\pi f_{ac}n)\sum_{n=n_0}^{n=n_1}\sin^2(2\pi f_{ac}n) - \Big(\sum_{n=n_0}^{n=n_1}\cos(2\pi f_{ac}n)\sin(2\pi f_{ac}n)\Big)^2\Big)\sum_{n=n_0}^{n=n_1}u_n. \end{aligned} \tag{50}$$

Similarly, the acoustic parameters express as

$$\begin{aligned} a_{ac} \;=\; & \frac{1}{N^3 D}\Big(\sum_{n=n_0}^{n=n_1}\sin^2(2\pi f_{ac}n)\Big(\sum_{n=n_0}^{n=n_1}\sin(2\pi f_{ac}n)\Big)^2\Big)\sum_{n=n_0}^{n=n_1}u_n\cos(2\pi f_{ac}n) \\ & +\frac{1}{N^3 D}\Big(\sum_{n=n_0}^{n=n_1}\cos(2\pi f_{ac}n)\sum_{n=n_0}^{n=n_1}\sin(2\pi f_{ac}n) - \sum_{n=n_0}^{n=n_1}\cos(2\pi f_{ac}n)\sin(2\pi f_{ac}n)\Big)\sum_{n=n_0}^{n=n_1}u_n\sin(2\pi f_{ac}n) \end{aligned}$$

$$+\frac{1}{N^3D}\left(\sum_{n=n_0}^{n=n_1}\sin(2\pi f_{ac}n)\sum_{n=n_0}^{n=n_1}\cos(2\pi f_{ac}n)\sin(2\pi f_{ac}n)-\sum_{n=n_0}^{n=n_1}\cos(2\pi f_{ac}n)\sin^2(2\pi f_{ac}n)\right)\sum_{n=n_0}^{n=n_1}u_n, \quad (51)$$

and

$$\begin{aligned} b_{ac} &= \frac{1}{N^3D}\left(\sum_{n=n_0}^{n=n_1}\cos^2(2\pi f_{ac}n)\left(\sum_{n=n_0}^{n=n_1}\cos(2\pi f_{ac}n)\right)^2\right)\sum_{n=n_0}^{n=n_1}u_n\sin(2\pi f_{ac}n) \\ &+\frac{1}{N^3D}\left(\sum_{n=n_0}^{n=n_1}\cos(2\pi f_{ac}n)\sum_{n=n_0}^{n=n_1}\sin(2\pi f_{ac}n)-\sum_{n=n_0}^{n=n_1}\cos(2\pi f_{ac}n)\sin(2\pi f_{ac}n)\right)\sum_{n=n_0}^{n=n_1}u_n\cos(2\pi f_{ac}n) \\ &+\frac{1}{N^3D}\left(\sum_{n=n_0}^{n=n_1}\cos(2\pi f_{ac}n)\sum_{n=n_0}^{n=n_1}\cos(2\pi f_{ac}n)\sin(2\pi f_{ac}n)-\sum_{n=n_0}^{n=n_1}\sin(2\pi f_{ac}n)\cos^2(2\pi f_{ac}n)\right)\sum_{n=n_0}^{n=n_1}u_n. \end{aligned} \quad (52)$$

APPENDIX II

ASYMTOTIC CRB

In this Appendix, we write the CRB of v_c (25), V_{ac} (30) and ϕ_{ac} (31) respectively in both asymptotic cases

$$2\gamma N \ll 1, \quad (53)$$

and

$$2\gamma N \gg 1, \quad (54)$$

where γ and $N \equiv N_q$ are given by (22) and (36). Using (36) and (22), we note that (53) and (54) are respectively equivalent to

$$2\sqrt{2}\pi D_x F_{ac} \ll v_c, \quad (55)$$

and

$$2\sqrt{2}\pi D_x F_{ac} \gg v_c. \quad (56)$$

Firstly, we suppose that $2\gamma N \ll 1$ and that $\gamma \ll 1$ which means that the actual velocity signal corresponds to largely less than one acoustic period. The Taylor expansion at the 7th order of the sine functions in (25), (30) and (31) respectively yields

$$\text{var}(v_c) \geq \sigma^2 \frac{45}{\pi^4 f_{ac}^4}\frac{1}{N^5}, \quad (57)$$

$$\text{var}(V_{ac}) \geq \frac{\sigma^2}{2}\frac{45}{\pi^4 f_{ac}^4}\frac{1}{N^5}, \quad (58)$$

$$\text{var}(\phi_{ac}) \geq \frac{\sigma^2}{2V_{ac}^2}\frac{45}{\pi^4 f_{ac}^4}\frac{1}{N^5}. \quad (59)$$

Using (36) and (22), we note that (57-59) may respectively be written as

$$\mathrm{var}(v_c) \geq \sigma^2 \frac{45}{\pi^4 2^{5/2}} \frac{1}{D_x^5 F_e} \frac{v_c^5}{F_{ac}^4}, \tag{60}$$

$$\mathrm{var}(V_{ac}) \geq \sigma^2 \frac{45}{\pi^4 2^{7/2}} \frac{1}{D_x^5 F_e} \frac{v_c^5}{F_{ac}^4}, \tag{61}$$

$$\mathrm{var}(\phi_{ac}) \geq \sigma^2 \frac{45}{\pi^4 2^{7/2}} \frac{1}{D_x^5 F_e} \frac{v_c^5}{F_{ac}^4 V_{ac}^2}. \tag{62}$$

Writing (24) into (60-62) leads to

$$\mathrm{var}(v_c) \geq \frac{1}{\mathrm{SNR}} \frac{45}{\pi^4 2^{7/2}} \frac{1}{D_x^5 F_e} \frac{v_c^5 V_{ac}^2}{F_{ac}^4}, \tag{63}$$

$$\mathrm{var}(V_{ac}) \geq \frac{1}{\mathrm{SNR}} \frac{45}{\pi^4 2^{9/2}} \frac{1}{D_x^5 F_e} \frac{v_c^5 V_{ac}^2}{F_{ac}^4}, \tag{64}$$

$$\mathrm{var}(\phi_{ac}) \geq \frac{1}{\mathrm{SNR}} \frac{45}{\pi^4 2^{9/2}} \frac{1}{D_x^5 F_e} \frac{v_c^5}{F_{ac}^4}, \tag{65}$$

where SNR is the linear signal-to-noise ratio.

Secondly, we now suppose that $2\gamma N \gg 1$ which means that the actual velocity signal corresponds to largely great than one acoustic period. The asymptotic CRB is then such that

$$\mathrm{var}(v_c) \geq \frac{\sigma^2}{N}, \tag{66}$$

$$\mathrm{var}(V_{ac}) \geq \frac{2\sigma^2}{N} \tag{67}$$

and

$$\mathrm{var}(\phi_{ac}) \geq \frac{2\sigma^2}{N V_{ac}^2}. \tag{68}$$

Using (36), we note that (66-68) may respectively be written as

$$\mathrm{var}(v_c) \geq \frac{\sigma^2}{\sqrt{2} D_x F_e} v_c, \tag{69}$$

$$\mathrm{var}(V_{ac}) \geq \frac{\sqrt{2}\sigma^2}{D_x F_e} v_c \tag{70}$$

and

$$\mathrm{var}(\phi_{ac}) \geq \frac{\sqrt{2}\sigma^2}{D_x F_e}\frac{v_c}{V_{ac}^2}. \tag{71}$$

Lastly, inserting (24) into (69-71) finally leads to

$$\mathrm{var}(v_c) \geq \frac{1}{\mathrm{SNR}}\frac{1}{2^{3/2} D_x F_e} v_c V_{ac}^2, \tag{72}$$

$$\mathrm{var}(V_{ac}) \geq \frac{1}{\mathrm{SNR}}\frac{1}{\sqrt{2} D_x F_e} v_c V_{ac}^2 \tag{73}$$

and

$$\mathrm{var}(\phi_{ac}) \geq \frac{1}{\mathrm{SNR}}\frac{1}{\sqrt{2} D_x F_e} v_c \tag{74}$$

References

[1] H. E. Albrecht, N. Damaschke, M. Borys, and C. Tropea. *Laser Doppler and Phase Doppler Measurement Techniques*. Springer Verlag, 2003.

[2] R. Banning. Spectral analysis methods for poisson sampled measurements. *IEEE Trans. Instrum. Meas.*, **46**(4):882–887, 1997.

[3] O. Besson and F. Galtier. Estimating particles velocity from laser measurements: maximum likelihood and cramer-rao bounds. *IEEE Trans. Signal Proc.*, **44**(12):3056–3068, 1996.

[4] R. Boucheron, J.C. Valière, Ph. Herzog, H. Baillet, and J.P. Dalmont. Evaluation of acoustic velocity in mean flow by Laser Doppler Velocimetry. In *Proceedings of 12th International Symposium on Applications of Laser Techniques to fluid Mechanics*, Lisbon, Portugal, 2004.

[5] L. Boyer and G. Searby. Random sampling : distortion and reconstruction of velocity spectra from fft analysis of the analog signal of laser doppler processor. *J. Appl. Phys.*, **60**(8):2699–2707, 1986.

[6] M.R. Davis and K.J. Taylor. Laser Doppler measurement of complex impedance. *J. Sound Vib.*, **107**(3):451–470, 1986.

[7] A. Degroot, S. Montrésor, B. Gazengel, O. Richoux, and L. Simon. Doppler signal detection and particle time of flight estimation using wavelet transform for acoustic velocity measurement. In *ICASSP'2006 - IEEE International Conference on Acoustics Speech and Signal Processing*, Toulouse, France, 2006.

[8] B. Gazengel and S. Poggi. Measurement of acoustic particle velocities in enclosed sound field: Assessment of two laser doppler velocimetry measuring systems. *Applied Acoustics*, **66**(1):15–44, 2005.

[9] B. Gazengel, S. Poggi, and J.C. Valière. Evaluation of the performances of two acquisition and signal processing systems for measuring acoustic particle velocities in air by means of laser doppler velocimetry. *Meas. Sci. Tech.*, **14**(12):2047–2064, 2003.

[10] C.A. Greated. Measurement of acoustic velocity fields. *Strain*, **22**:21–24, 1986.

[11] E. Mller H. Nobach and C. Tropea. Efficient estimation of power spectral density from laser doppler anemometer data. *Exp. in Fluids*, **24**(5-6):499–509, 1998.

[12] S.M. Kay. *Fundamentals of statistical signal processing. Vol. I: estimation theory*. Prentice-Hall, 1993.

[13] Z. Lazreq and J.M. Ville. Acoustic calibration of a pressure-velocity probe. *J. Acoust. Soc. Am.*, **100**(1):364–371, 1996.

[14] A. Le Duff, G. Plantier, J.C. Valière, and R. Perdriau. Particle detection and velocity measurements in laser doppler velocimetry using Kalman filters. In *ICASSP'2004 - IEEE International Conference on Acoustics Speech and Signal Processing*, Montréal, Québec, 2004.

[15] A. Minotti, F. Simon, J.F. Piet, and P. Millan. In-flow acoustic power and intensity field measurements with a 2D LDV system. In *AIAA/CEAS Aeroacoustic conference AIAA 2003-3262*, Hilton Head, 2003.

[16] W.K. George P. Buchhave and J.L. Lumley. The measurement of turbulence with the laser-doppler anemometer. *Ann. Rev. Fluid. Mech.*, **11**:443–503, 1979.

[17] D. Rife and R. Boorstyn. Single tone parameter estimation from discrete-time observations. *IEEE Trans. Info. Theory*, **20**(5):591–598, 1974.

[18] J.P. Sharped and C.A. Greated. A stochastic model for photon correlation measurements in sound field. *J. Phys. D:Appl. Phys.*, **22**:1429–1433, 1989.

[19] W.Q. Shu. Cramer-rao bound of laser doppler anemometer. *IEEE Trans. Instrum. Meas.*, **50**(6):1770–1772, 2001.

[20] L. Simon and J. Fitzpatrick. An improved sample-and-hold reconstruction procedure for auto-power spectra estimation of lda data. *Exp. in Fluids*, **37**(2):272–280, 2004.

[21] K.J. Taylor. Absolute measurement of acoustic particle velocity. *J. Acoust. Soc. Am.*, **59**:691–694, 1976.

[22] K.J. Taylor. Absolute calibration of microphone by Laser Doppler technique. *J. Acoust. Soc. Am.*, **70**(4):939–945, 1981.

[23] V. Valeau, J.C. Valière, and C. Mellet. Instantaneous frequency tracking of a sinusoidally frequency-modulated signal with low modulation index: application to laser measurements in acoustics. *Sig. Proc.*, **84**(7):1147–1165, 2004.

[24] J.C. Valière, P. Herzog, V. Valeau, and G. Tournois. Acoustic velocity measurements in the air by means of laser doppler velocimetry : dynamic and frequency range limitations and signal processing improvements. *J. Sound Vib.*, **229**(3):607–626, 2000.

[25] J.F. Vignola, Y.H. Berthelot, and J. Jarzinsjy. Laser detection of sound. *J. Acoust. Soc. Am.*, **90**:1275–1286, 1991.